

Edge spin wave transmission through a vertex domain wall in triangular dots

Diego Caso¹ and Farkhad Aliev^{1,2}

¹Departamento de Física de la Materia Condensada C03, Universidad Autónoma de Madrid, Cantoblanco, Madrid, 28049, Spain.

² Instituto Nicolás Cabrera (INC) and Condensed Matter Physics Institute (IFIMAC), Universidad Autónoma de Madrid, Cantoblanco, Madrid, 28049, Spain.

Contributing authors: diego.caso@uam.es; farkhad.aliev@uam.es;

Abstract

Spin waves (SWs), being usually reflected by domain walls, could also be channeled along them. Edge domain walls yield the interesting, and potentially applicable to real devices property of broadband spin waves confinement to the edges of the structure. Here we investigate through numerical simulations the propagation of quasi one-dimensional spin waves in triangle-shaped amorphous YIG ($\mathbf{Y}_3\mathbf{Fe}_5\mathbf{O}_{12}$) micron sized ferromagnets as a function of the angle aperture. The edge spin waves (ESWs) have been propagated over the corner in triangles of 2 microns side with a fixed thickness of 85 nm. Parameters such as superior vertex angle (in the range of 40°-75°) and applied magnetic field have been optimized in order to obtain a higher transmission coefficient of the ESWs over the triangle vertex. We observed that for a certain aperture angle for which dominated ESW frequency coincides with one of the localised DW modes, the transmission is maximized near one and the phase shift drops to $\pi/2$ indicating resonant transmission of ESWs through the upper corner. We compare the obtained results with existing theoretical models. These results could contribute to the development of novel basic elements for spin wave computing.

1 Introduction

Despite the growing success of magnonics in recent years, particularly due to its potential application for spin wave computing and signal processing [1], the currently available spin-wave devices based on ferromagnetic strip lines are limited in the frequency span and have none or limited capability in the redirection of SWs [1, 2]. Their typical operating frequencies are below few GHz, and the propagation is confined to linear coplanar waveguides. Magnon excitation is usually achieved through coupling between the magnetization and the magnetic field due to microwave (mw) currents. The field is however difficult to confine to sub-micrometre volumes. This impedes the use of the traditional inductive coupling methods. Lara et al. [3] proposed a technologically new approach which could lead to a radical enhancement of the coupling in small magnonics structures, ultimately promising a full integration of the SW devices into CMOS technology.

This radically new pathway is based on the excitation and propagation of a new class of localized quasi-one-dimensional spin waves, the so called Winter magnons (WMs) [4]. These spin waves are analogous to the displacement waves of strings and could be excited in a wide class of patterned magnetic nanostructures possessing domain walls (DWs). Localized WMs have been identified experimentally in different ferromagnetic structures with domain walls. Winter magnons have been excited in circular magnetic dots in double vortex states, being localized along DWs connecting vortex cores with half-antivortices [5]. The experiments have been supported by numerical modelling and analytical theory. Garcia-Sanchez et al. [6] evidenced theoretically and through micromagnetic simulations non-reciprocal channeling of WMs in ultrathin ferromagnetic films along Néel-type DWs arising from a Dzyaloshinskii-Moriya (DMI) interaction. A possible application of WMs propagated along DWs regarding their use as reconfigurable spin-wave nanochannels was suggested by Wagner et al. [7]. Park et al. [8] and Osuna Ruiz et al. [9] investigated the propagation of WMs in patterned structures involving both DWs and single vortex states. Also, WMs excited in exchange-coupled ferromagnetic bilayers have been proposed for their implementation in emerging spin wave logic and computational circuits [10].

Lara et al. were first to propose the excitation of WMs along the edges of the device [11]. This entirely different proposal of transmission uses WMs confined to edge DWs in ferromagnetic geometries such as triangles or rectangles in configurations created by an in-plane (IP) bias field [3]. The resulting state indeed supports the excitation and detection of SWs locally in magnonic logic gates, leading to a natural decrease in device dimensions. Control over edge-localized SWs was accomplished by Zang et al. by placing magnetic structures adjacently to a propagating microstrip [12]. Additionally, micromagnetic simulations done by Gruszecki et al. demonstrated that the edge of a structure with locally confined SWs could be used to excite plane waves with twice its frequency and less than half its wavelength [13].

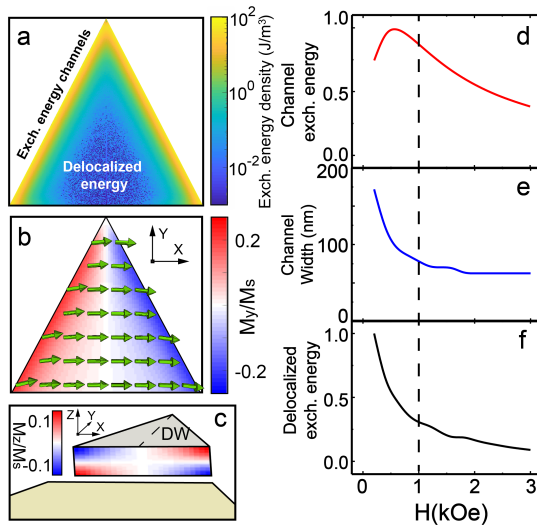


Fig. 1 (a) Shows the exchange energy density distribution of the YIG triangle with an applied 1 kOe IP magnetic field parallel to the base of the geometry. Exchange energy is accumulated on the lateral edges of the triangle, creating exchange energy channels of ESW propagation. (b) Illustrates an enhancement of the soft DW static head-to-tail bulk magnetic configuration before any mw excitation. When far from the surface, the DW has an almost completely Néel-type configuration. However, the out-of-plane (OOP) component increases in regions closer to the surface (c). (d) Indicates how the exchange energy density of the channel behaves with the intensity of the applied field, evaluated from a cross section at the middle of the triangle. This is maximized at 800 Oe before it decays. (e) Is a measure of the exchange energy channel width vs the applied field. The channel boundary is taken as a 90 % decrease of the highest exchange energy of the channel. With more applied field the channel is being narrowed, which implies a better localization of the ESW propagation. (f) Shows how the exchange energy outside the channel (delocalized exchange energy) also decreases with field, which implies that the spin wave will be less likely to travel through the non-edge region of the triangle and cause interferences on the other side

Our work investigates numerically the excitation, propagation and control of edge spin waves in micron sized YIG triangles with different apertures. We have observed resonant enhancement of ESW transmission for certain aperture angles accompanied by a $\pi/2$ phase shift of the propagated spin wave. We link this effect to the interaction of the surface spin waves with the vertex domain wall.

2 Results and Discussion

2.1 Optimization of the exchange energy channels with applied bias field

To get the ground state magnetization distribution a static bias field is applied parallel to the base of the triangle. Once the system is relaxed, the exchange energy distribution will be similar to Fig. 1(a). Depending on the strength of the magnetic field, the exchange energy will be accumulated in a larger or

lesser capacity in the lateral edges of the triangle, shaping two exchange energy channels ([3]). Fig. 1(b) and Fig. 1(d) both allude to this phenomena: for small fields the exchange energy progressively transfers from being delocalized to being part of the exchange energy channels. Logically, when stronger field is applied there is also a better localization of the exchange energy on the edges (Fig. 1(c)). For higher fields however, the exchange energy localized in the edges and the delocalized energy both drop. This results in a weakening of the channels, which is not desirable for SW propagation. Hence, we chose to use 1 kOe for our micromagnetic simulations, this field results in channels of propagation with high exchange energy and well localized in the edge of the triangle. Relaxing the magnetic system with no applied field yields in a configuration with an excess of exchange energy as a perpendicular barrier from the middle of the triangles base up to the top corner, which could potentially also be used to propagate SWs. When the 1kOe IP field is applied and the system is relaxed, the remnants of this barrier survive in the top corner. This is related to a DW that is originated in the top corner in this particular configuration.

After the bias field is applied and the system is relaxed, the static magnetization distribution is mostly IP saturated in the direction of the field. However, close to the edges of the triangle the magnetization becomes increasingly parallel to them due to the minimization of stray fields. In the upper corner, this translates as a complete change of the IP magnetization component perpendicular to the base (Y axis) from one side to another of the triangle, leading to a soft 30° Néel-type domain wall (DW) in the top vertex. However, this is an accurate assessment only in the bulk of the structure, since the magnetization has an increasing out-of-plane (OOP) component in the surfaces of the triangle (see Fig. 1c), leading to a state were the DW minimum-energy configuration is intermediate between Bloch and Néel. The resulting state is close to having a weak DMI-like effect [14]. This topological anomaly has in itself its own magnetic texture and it is of interest to understand spin wave propagation through such structures. The DW spin configuration is head-to-tail, however, extreme high-reflection and low-transmission effects that would occur in 90° Néel-type head-to-tail DWs are negligible due to the softness of the DW, leading to an almost transparent structure in terms of transmission [15]. The width of the DW is measured at ~ 180 nm.

2.2 Propagation of the Edge Spin Waves

The generated DW has its own associated eigenmodes that can be dynamically stimulated, this is key to understand SW transmission and further effects that will be discussed later on. After a 20 ns sinc-shaped pulse (see Methods), we found that the response of the whole system to the pulse resulted in clear distinguishable eigenmodes (bulk modes from now on) for all of the analyzed angles (in the 35-70 degrees range of top corner angle) from 3 GHz to 5 GHz (see Fig. 2a). The mode of the highest amplitude, however, is closer to 4.4 GHz, slightly oscillating for the different triangle apertures (Fig. 2b).

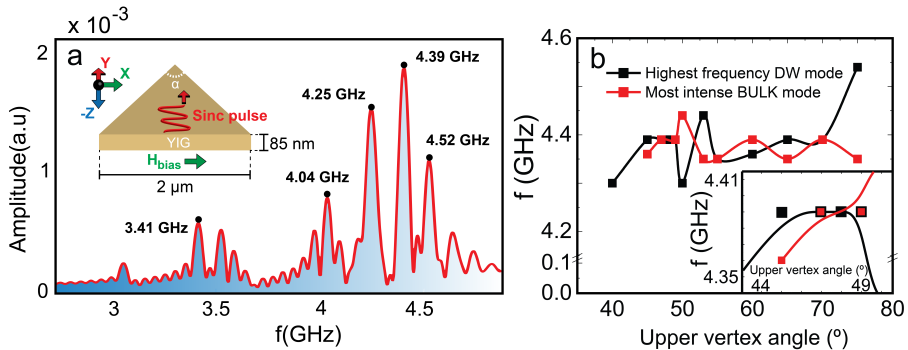


Fig. 2 (a) Average modes of the whole YIG triangle's OOP magnetization component visualized in the particular case of a 49° aperture. The most intense mode (in this case 4.39 GHz) is to be excited in the left corner of the triangle. Inset shows a sketch of magnetic field distribution in the system: a 1 kOe DC field parallel to the base of the triangle and a smaller AC pulse perpendicular to it. (b) Frequency of the mode with the highest frequency in the DW and the most intense bulk mode against the angle aperture. For a wide range of angles in the high transmission region or fairly close to it, some DW modes frequencies agree with bulk modes, i.e., when exciting with this frequency they couple and result on a resonant system, which amplifies the transmission through the DW

The analysis of the eigenfrequencies is also done for local known specific magnetic structures such as the edges or the upper vertex DW. This allows to differentiate the propagation of the spin waves through three different magnetic structures with their own modes: bulk, edges, and the DW. Local analysis of the eigenmodes displays that generally $f(\text{bulk}) > f(\text{edges}) > f(\text{DW})$ (f being the frequency of the modes). However, these modes are not overwhelmingly separated (all of them are between 1 and 5 GHz), and one can exploit this fact to excite the system at matching frequencies between two -or more- of these structures, resulting in a resonance-like system in which energy is being pumped from the magnetic structures to the spin wave to keep the propagation going.

Local excitation of the spin waves is done at the left corner of the triangle, where the magnetization is conflicted between being parallel to the left edge or to the base, which is the bulk magnetization direction. Because there is no inherent symmetry in the magnetic display of the system, the results found cannot be generalized to the right corner of the triangle, i.e., to an anti-parallel configuration of the magnetization in the bulk. The used frequency for the mw excitations are the most intense detected bulk modes. However, this excitations are directed effectively perpendicular to the left edge of the triangle. Thanks to this and to the exchange energy channels we can "trick" the spin wave to being almost completely localized in the edges of the system (see insert of Fig. 3a), even though the excited modes are present in the whole system.

Spin waves propagated from the left to the right corner of the triangle (see Supplementary videos) show a range of aperture angles in which there is a peak in transmission, even slightly surpassing the value of 1 for 49° , which means the spin wave is more intense in the right side of the triangle (see Fig. 3a). The

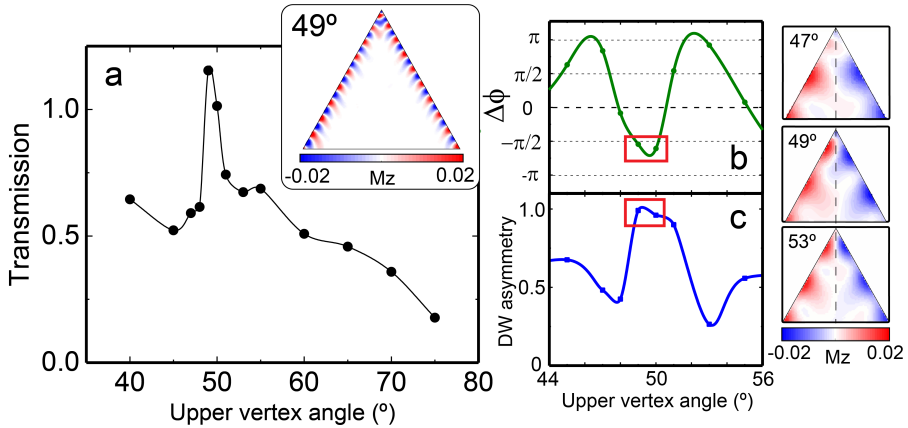


Fig. 3 (a) Transmission coefficient of the ESW for an upper vertex angle aperture between 40 and 75 degrees analyzed in the bulk of the triangle. The distinct transmission peak at 49-50° indicates that the spin wave propagates almost perfectly through the edges of the triangle. Inset shows the ESW propagating through the edges for 49 degree angle. The excited frequencies correspond in each case for the most intense bulk mode. (b) Phase shift of the ESW induced at the upper vertex DW. At the 49-50° aperture angle, which is the high transmission range, the ESW experiences a $\pi/2$ phase shift, which indicates the possible existence of resonance. (c) DW asymmetry between the two lateral sides of the triangle in the propagation of the ESW indicates a more asymmetrical propagation for the high transmission angles. Inset reveals an enhancement of the upper vertex DW to show the propagation pattern of three different angles

high dependence in SW transmission with the aperture angle remarks that the upper vertex DW topology is highly important in the process. Such increment in transmission of the SWs in a narrow range of top corner aperture angle is a simultaneous effect to the fact that the excited most intense bulk modes match the highest frequency eigenmodes found in for the DW (see Fig. 2b). This correlation is very difficult to disregard, and backs up the expected result in a resonant system with two sources. A deep analysis of the process in the upper vertex DW when the SW is propagated helps to understand this effects: for the high transmission angle range, the SWs experiments a phase shift close to $\pi/2$ (marked in red in Fig. 3b), which is in agreement with some mechanical systems in resonance and previous recorded phase-shifts in Néel-type DWs [16].

The calculated DW asymmetry along an axis parallel to the Y axis that divides the upper vertex in two (see insert of Fig. 3c) is also maximum for the angles of high transmission coefficient, which is highly correlated to the $\pi/2$ phase shift (Fig. 3c). At 49° (see insert of Fig. 3c), the incoming and departing signals at the corner almost completely wrap up one another (which happens due to the $\pi/2$ phase shift) and therefore are not disturbed by each other, showing the high efficiency of the local DW SW propagation for this angles. However, for an angle outside of the high transmission range this is not true and the incoming and departing SWs are in each others way, resulting in a transmission not as efficient.

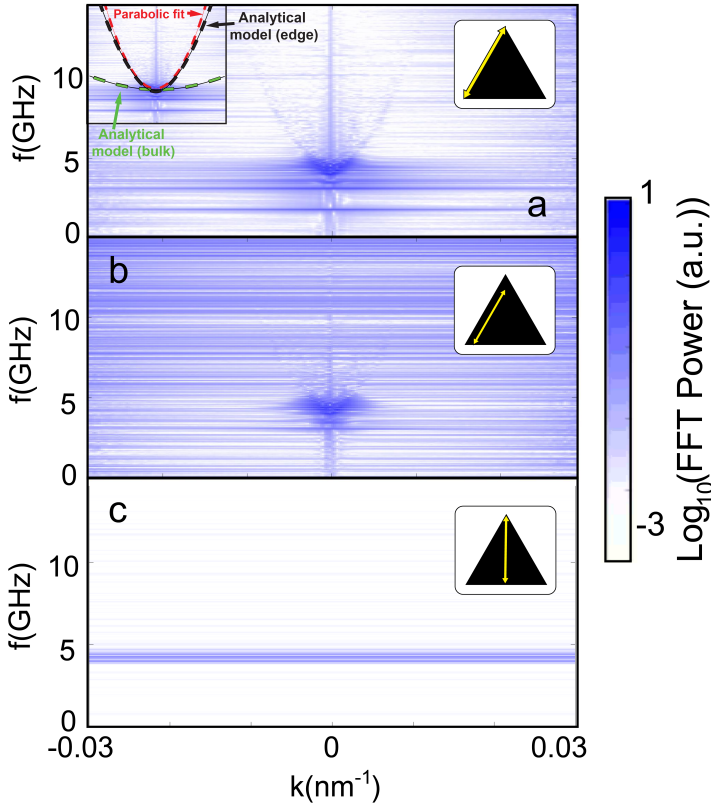


Fig. 4 Dispersion relation in a 49 degree angle aperture triangle for (a) the left edge of the triangle from the left vertex all the way to the top. Both dynamical regimes are represented in the chosen path: the low-frequency modes constant in frequency and the parabolic ones, at higher frequencies. (b) The left side of the dot with a separation of $\sim 80nm$ from the edge. Although noticeable, both mode regimes are less intense than in the case of the left edge analysis. (c) A straight line perpendicular to the base of the dot, separating it in two halves. In this particular case only the low-frequency modes are present. These results reveal a direct correlation between the low frequency modes and the top corner of the triangle, associated with the DW, and the parabolic mode with the edge of the system

2.2.1 Dispersion Relations

Analyzed SW dispersion reveals two different dynamic regimes: low-frequency modes, which are constant in frequency along all wavenumbers, and a parabolic mode at higher frequencies (see Fig. 4a). This regimes are both present when the dispersion is represented from the data obtained in the edge region. Different performed tests reveal that the intensity of the dynamic regimes is dependant on the path chosen for the 2D Fourier Transform analysis, which generates the dispersion relations: a path that crosses through the left edge of the structure is associated with the two dynamic regimes being present (Fig. 4a). However, they become less intense if the path is separated from the edges (see Fig. 4b). If the path crosses the triangle from the base all the way to the

upper vertex the dispersion relation only shows the constant frequency modes through all wavenumbers (see Fig. 4c). This constitutes enough evidence to assert that the low frequency modes are localized DW-related modes, and the parabolic mode is linked to ESWs. Here, the positive k vector branch of the parabolic mode corresponds to the ESWs emitted by the left vertex while the negative k branch describes ESWs emitted by the top corner in direction to the left vertex. In this configuration, these two branches have an equivalent intensity, meaning that the propagation of ESWs is as easy in both directions.

Their approximately parabolic dispersion relation also corroborates the predominantly 1D character of SWs along the edge with an IP field parallel to the base. Indeed, the exact solution for SDWs in a 1D ferromagnetic chain predicts a parabolic k dispersion [17], valid except in the region of $k \rightarrow 0$, where the dipolar contribution dominates. The parabolic nature of the dispersion relation of the ESWs also matches the expected for the analytical model proposed by Lara et al. [3] if the exchange length in the edges is more (an order of magnitude) than the expected value at the bulk (see insert of Fig. 4a). This is reasonable since the exchange energy is predominantly accumulated in the edges, which would generate a stronger coupling of the magnetic moments in this region, and thus, a longer coupling distance.

2.3 Theoretical models

Several studies have previously considered theoretically spin wave propagation through a domain wall. Hertel et al. [19] predicted that there is a proportionality between the SW phase shifted produced by DW and the angle by which the magnetization rotates inside this domain wall ($\Delta\phi = \Delta f/2$), meaning that the phase of spin waves with k -vector perpendicular to a domain wall changes by a factor of $\pi/2$ when the wave propagates in a ferromagnetic layer through a transverse wall. The changes of the phase shift of the spin wave with upper vertex aperture angle observed here suggests a possible topological variability of DW magnetic texture with angle aperture once the excitation reaches a steady state, as confirmed by our results. However the model [19] also suggests that at the high transmission range, in which the phase shift is almost exactly $\pi/2$, the DW becomes completely transverse. This scenario must be discarded due to the analysis done at the DW, which does not show a situation with a particularly hard DW, even when the spin wave is stabilized.

On the other hand, Bayer et al. [20] predicted analytically that the spin-wave transport through an infinitely extended one-dimensional Bloch-type domain wall induces a finite phase shift without reflection. We deduce then that the slight OOP component in the DW plays a role in the transmission of the wave. Indeed, when the excitation stabilizes, the spin wave propagating on each side of the dot have opposed OOP component, meaning that is key for the energy minimization in the system. Further studies involving more precise control over magnetic texture of the vertex domain wall, for example

using underlying material with spin orbit coupling (for example a *Pt* underlayer) are needed to explore the direct link between the vertex DW internal magnetic texture and the spin wave transmission through it.

3 Conclusions

Detailed investigation of the influence of the upper vertex aperture on transmission and dephasing of edge spin waves in amorphous YIG ferromagnetic triangles shows the possibility of fine tuning of the edge spin wave transmission between two remote corners. The results suggest that 49-50° of the aperture angle triggers a high transmission response of the spin wave propagation system. Local analysis of the eigenmodes reveals following relation: $f(\text{bulk}) > f(\text{edges}) > f(\text{DW})$ for the vast majority of those SW modes branches. In some instances, however, the local modes seemly overlap each other, resulting in an energy pumping into the upper vertex DW structure. The maximum DW asymmetry is found at the high transmission range, as well as a phase shift of $\pi/2$, characteristic of resonant systems and Néel-type DWs. The analysis of the SW dispersion relations reveal that the DW-related modes are constant in frequency, whereas the ESWs modes have a parabolic behavior. The best fit to the analytical model [3] suggests a possible increase of the exchange length along the edge DW. We conclude that the high transmission mechanism is greatly due to the specific DW topology on each angle aperture, which could indeed raise resonance-like interactions between local and bulk SW modes in the triangular ferromagnetic structure. We believe that this work could contribute to better understand the SW propagation through topological objects and/or magnetic textures.

Methods The micromagnetic simulations were carried out using the MuMax3 code [18]. The typical YIG parameters were used: saturation magnetization $M_s = 130$ kA/m, exchange stiffness constant $A_{ex} = 3.5 \times 10^{-12}$ J/m and damping constant $\alpha = 2.8 \times 10^{-3}$. The base of the used triangles was $2 \mu\text{m}$ and its thickness 85 nm. Discretization was set at $7.8 \times 6.7 \times 4.2$ nm per cell ($256 \times 256 \times 20$ cells) for a standard 60° angle triangle, enough to precisely characterize the upper vertex DW. No anisotropies were added to our structure. To find the eigenfrequencies of a magnetic system, a 2 Oe, 20 ns, sinc-shaped in-plane magnetic field pulse was applied uniformly perpendicularly to both the base of the triangle and the direction of the applied static field. After relaxing the system, the spin wave eigenmode spectrum is obtained using the Fourier Transform of the OOP component of the magnetization. Knowing the eigenfrequencies, which appear as peaks in the absorption spectrum, a local excitation at a single eigenfrequency can be applied to observe the response of the magnetic (i.e., to observe the propagation of spin waves away from the source), for as long as it may be necessary for the spin waves to reach a target area. Dispersion relations are calculated from the simulations using a 2D Fourier Transform of the magnetization along a desired path.

Acknowledgments Authors acknowledge Ahmad Awad and César González-Ruano for discussions. The work in Madrid was supported by Spanish Ministerio de Ciencia (RTI2018-095303-B-C55) and Consejería de Educación e Investigación de la Comunidad de Madrid (NANOMAGCOST-CM Ref. P2018/NMT-4321) Grants. FGA acknowledges financial support from the Spanish Ministry of Science and Innovation, through the "María de Maeztu" Program for Units of Excellence in *R&D* (CEX2018-000805-M) and "Acción financiada por la Comunidad de Madrid en el marco del convenio plurianual con la Universidad Autónoma de Madrid en Línea 3: Excelencia para el Profesorado Universitario". D.C. has been supported by Comunidad de Madrid by contract through Consejería de Ciencia, Universidades e Investigación y Fondo Social Europeo (PEJ-2018-AI/IND-10364)

References

- [1] A. V. Chumak, et al (2021) Roadmap on spin-wave computing. *Cond. Mat.* ArXiv: 2111.00365. Submitted to IEEE Transactions on Magnetics.
- [2] A. V. Chumak, A. A. Serga, B. Hillebrands (2017) Magnonic crystals for data processing. *J Phys D: Appl Phys* 50:244001. <https://doi.org/10.1088/1361-6463/aa6a65>
- [3] A. Lara, J. R. Moreno, K.Y. Guslienko, F. G. Aliev (2017) Information processing in patterned magnetic nanostructures with edge spin waves. *Sci Rep*, 7:5597 <https://doi.org/10.1038/s41598-017-05737-8>
- [4] J. M. Winter (1961) Bloch wall excitation. Application to nuclear resonance in a Bloch wall. *Phys Rev* 124:452–459 <https://doi.org/10.1103/PhysRev.124.452>
- [5] F. G. Aliev, A. A. Awad, D. Dieleman, A. Lara, V. Metlushko, K. Y. Guslienko (2011) Localized domain-wall excitations in patterned magnetic dots probed by broadband ferromagnetic resonance. *Phys Rev B* 84:224511 <https://doi.org/10.1103/PhysRevB.84.144406>
- [6] F. Garcia-Sanchez, P. Borys, R. Soucaille, J. Adam, R. L. Stamps, J. Kim (2015) Narrow magnonic waveguides based on domain walls. *Phys Rev Lett* 114:247206 <https://doi.org/10.1103/PhysRevLett.114.247206>
- [7] K. Wagner, A. Kákay, K. Schultheiss, A. Henschke, T. Sebastian, H. Schultheiss (2016) Magnetic domain walls as reconfigurable spin-wave nanochannels. *Nature Nanotech* 11:432–436 <https://doi.org/10.1038/nnano.2015.339>
- [8] H. Park, J. Lee, J. Yang, S. Kim (2020) Interaction of spin waves propagating along narrow domain walls with a magnetic vortex in a

- thin-film-nanostrip cross-structure. *Journal of Applied Physics* 127:183906
<https://doi.org/10.1063/5.0005118>
- [9] D. Osuna Ruiz, E. Burgos Parra, N. Bukin, M. Heath, A. Lara, F. G. Aliev, A. P. Hibbins, F. Y. Ogrin (2019) Dynamics of spiral spin waves in magnetic nanopatches: Influence of thickness and shape. *Phys. Rev. B* 100:214437 <https://doi.org/10.1103/PhysRevB.100.214437>
- [10] V. Sluka, T. Schneider, R.A. Gallardo et al (2019) Emission and propagation of 1D and 2D spin waves with nanoscale wavelengths in anisotropic spin textures. *Nat Nanotechnol* 14:328–333
<https://doi.org/10.1038/s41565-019-0383-4>
- [11] A. Lara, V. Metlushko, F. G. Aliev (2013) Observation of propagating edge spin waves modes. *Journal of Applied Physics*, 114:213905
<https://doi.org/10.1063/1.4839315>
- [12] Z. Zhang, M. Vogel, M. B. Jungfleisch, A. Hoffmann, Y. Nie, V. Novosad (2019) Tuning edge-localized spin waves in magnetic microstrips by proximate magnetic structures. *Phys Rev B* 100:174434
<https://doi.org/10.1103/PhysRevB.100.174434>
- [13] P. Gruszecki, I. L. Lyubchanskii, K. Y. Guslienko, M. Krawczyk (2021) Local non-linear excitation of sub-100 nm bulk-type spin waves by edge-localized spin waves in magnetic films. *Appl Phys Lett* 118:062408
<https://doi.org/10.1063/5.0041030>
- [14] F.J. Buijnsters, Y. Ferreiros, A. Fasolino, M.I. Katsnelson (2016) Chirality-dependent transmission of spin waves through domain walls. *Phys Rev Lett* 116:147204 <https://doi.org/10.1103/PhysRevLett.116.147204>
- [15] S. J. Hämäläinen, M. Madami, H. Qin, G. Gubbiotti, S.V. Dijken (2018) Control of spin-wave transmission by a programmable domain wall. *Nat Commun* 9:1 <https://doi.org/10.1038/s41467-018-07372-x>
- [16] O. Wojewoda et al (2020) Propagation of spin waves through a Néel domain wall. *Appl Phys Lett* 117:022405
<https://doi.org/10.1063/5.0013692>
- [17] G. Gruner (1994) The dynamics of spin-density waves. *Rev Mod Phys* 66:1 <https://doi.org/10.1103/RevModPhys.66.1>
- [18] A. Vansteenkiste, J. Leliaert, M. Dvornik, M. Helsen, F. Garcia-Sanchez, B. V. Waeyenberge (2014) The design and verification of MuMax3. *AIP Advances* 4:107133 <https://doi.org/10.1063/1.4899186>

- [19] R. Hertel, W. Wulfhekel, J. Kirschner (2004) Domain-wall induced phase shifts in spin waves. *Physical Review Letters* 93:257202 <https://doi.org/10.1103/PhysRevLett.93.257202>
- [20] C. Bayer, H. Schultheiss, B. Hillebrands, R. Stamps (2005) Phase shift of spin waves traveling through a 180° bloch domain wall. *IEEE Transactions on Magnetics* 41:10 <https://doi.org/10.1109/TMAG.2005.855233>
- [21] A. V. Chumak, V. I. Vasyuchka, A. A. Serga, B. Hillebrands (2015) Magnon Spintronics. *Nature Phys* 11:453–461 <https://doi.org/10.1038/nphys3347>
- [22] C. Liu et al (2018) Long-distance propagation of short-wavelength spin waves. *Nat Commun* 9:738 <https://doi.org/10.1038/s41467-018-03199-8>
- [23] S. Macke, D. Goll (2010) Transmission and reflection of spin waves in the presence of Néel walls. *J Phys: Conf Ser* 200:042015
- [24] M. P. Kostylev, A. A. Serga, T. Schneider, T. Neumann, B. Leven, B. Hillebrands, R. L. Stamps (2007) Resonant and nonresonant scattering of dipole-dominated spin waves from a region of inhomogeneous magnetic field in a ferromagnetic film. *Phys Rev B* 76:184419 <https://doi.org/10.1103/PhysRevB.76.184419>